

Magnetic, specific-heat, and resistivity measurements of alloys $\text{CePd}_{2-x+y}\text{Mn}_x\text{Si}_{2-y}$ ($0 \leq x \leq 2$, $-0.1 \leq y \leq 0.1$)

B. Rupp and P. Rogl

Institut für Physikalische Chemie, University of Vienna, Währingerstrasse 42, A-1090 Vienna, Austria

N. Pillmayr, G. Hilscher, and G. Schaudy

Institut für Experimentalphysik, Technische Universität Vienna, Wiedner Hauptstrasse 8-10, A-1040 Vienna, Austria

I. Felner

Racah Institute of Physics, The Hebrew University, IL-91904 Jerusalem, Israel

(Received 15 February 1989; revised manuscript received 20 November 1989)

Measurements of (a) the lattice parameters at room temperature, (b) the magnetic susceptibility in the temperature range $1.5 \text{ K} < T < 300 \text{ K}$, (c) the electrical resistivity from 4.2 to 300 K, and (d) the specific heat from 1.5 to 60 K have been performed on the pseudobinary system $\text{CePd}_{2-x}\text{Mn}_x\text{Si}_2$. In the intermediate concentration range the character of the magnetic behavior changes from $4f$ magnetism—due to the Ce magnetic moments oriented in the $[110]$ direction in the Kondo-lattice system CePd_2Si_2 —to $3d$ magnetism in the $[001]$ direction carried by the Mn atoms without a magnetic moment at the Ce sites for CeMn_2Si_2 . Both boundary compounds crystallize with ThCr_2Si_2 structure and order antiferromagnetically at 10 and 379 K, respectively. The γ values of the electronic specific heat show a strong enhancement in the intermediate composition range where the change of the magnetic character occurs; this points (together with a reduction of the entropy for CePd_2Si_2 at T_N) to the appearance of spin fluctuations and/or Kondo scattering with screening of the Ce moments. Furthermore the Néel temperatures and the γ values sensitively depend upon the stoichiometry y in $\text{CePd}_{2+y}\text{Si}_{2-y}$.

I. INTRODUCTION

The magnetic properties in ternary cerium compounds CeT_2X_2 (T =transition metals, X =B, Si, P, Ge) with ThCr_2Si_2 ($I4/mmm$)—or the closely related CaBe_2Ge_2 ($P4/nmm$)-type structure—have recently attracted growing interest.^{1–5} The puzzling effects of valence fluctuation and Kondo-type coupling on the magnetic ordering were studied in $\text{Ce}(\text{Rh}, \text{Pd}, \text{Ag}, \text{Au})_2\text{Si}_2$ compounds (Refs. 1, 2, and 3). In these as well as in most cases CeT_2Si_2 (T =Fe, Co, Ni, Cu, Ru, Rh, Pd, Ag, Os, Ir, Pt, Au) valence fluctuation and/or magnetic ordering effects are both carried by the Ce atoms and ordering on the transition metal can be ruled out.^{6,7} Isotypic rare earth and actinoid manganese silicides with the ThCr_2Si_2 type, such as CeMn_2Si_2 , exhibit magnetic ordering characterized by strong ferromagnetic Mn-Mn interactions within the Mn layers and with a $(+ - + -)$ antiferromagnetic (AF) stacking sequence along the c axis^{8,9,10} leading to antiferromagnetic behavior by an AF coupling between the neighboring layers. In contrast to the rather restricted substitution of silicon by boron in CeT_2X_2 alloys,^{5,11} a transition-metal exchange in isotypic silicides generally resulted in the formation of extended solid solutions.^{12,13}

In particular, our interest was attracted by the CePd_2Si_2 - CeMn_2Si_2 pseudobinary system due to a possible valence transition and the interplay between $3d$ and $4f$ magnetism. The magnetic ordering in CePd_2Si_2 occurs on the Ce site solely with moments ordered antiparallel in the $[110]$ direction, whereas in CeMn_2Si_2 the magnetic ordering is carried by the Mn atoms with anti-

ferromagnetic stacking parallel to the c axis.

According to a recently attempted characterization¹⁴ of Ce compounds, CePd_2Si_2 was reported to belong to the so-called “Kondo regime,” where the interplay of $4f$ magnetism and Kondo-effect-type spin-fluctuation phenomena is typical. For the CeMn_2Si_2 low-energy scale, Ce valence mixing was shown^{15,16} to coexist with the high-energy scale $3d$ magnetism; as a consequence CeMn_2Si_2 was grouped into the so-called “intermediate regime”¹⁴ of mixed-valence Ce-alloy systems. Mn-Cr substitution in the coherent mixed-valent regime of CeMn_2Si_2 (Ref. 16) was found to induce a noncoherent Kondo-heavy-fermion Ce state. The present paper studies the system CePd_2Si_2 - CeMn_2Si_2 , in particular the interesting transition from a Ce Kondo regime to a Ce mixed-valent state coupled with a strongly magnetic $3d$ sublattice system.

II. EXPERIMENT

All samples, each of a total weight of 1 g were prepared by arc melting the elements together on a water-cooled copper hearth using a nonconsumable 2% thoriated tungsten electrode in Zr gettered high-purity argon. Starting materials were filings from cerium ingots (99.99% purity, Rare Earth Products, Ltd., U.K.), palladium and platinum powders (99.9%, Engelhard Ind. Div., USA), Ag powder (99.9%, Fluka, Switzerland), and crystallized 5N silicon powder (Alfa Ventron, FRG). Electrolyte manganese (99.9%, Fluka, Switzerland) was obtained in the form of plates, which were surface cleaned in dilute HNO_3 prior to use. Weight losses due

TABLE I. Unit-cell parameters and magnetic data of $\text{Ce}(T_1, T_2)_2\text{Si}_2$ alloys ($T_1 = \text{Pd}$, $T_2 = \text{Mn}$) with the ThCr_2Si_2 type of structure. The asterisk denotes this work. XRD stands for x-ray diffraction and ND stands for neutron diffraction.

Alloy composition	a_0 (Å)	c_0 (Å)	V_{uc} (Å ³)	c_0/a_0	T_N (K)	Θ_p (K)	$\mu_{\text{para}}^{\text{mol}}(\mu_B)$	Remarks	Reference
CePd_2Si_2	4.2367(10)	9.8880(16)	177.49	2.334		-19	2.31		Hiebl <i>et al.</i> (5)
	4.212	9.98	177.1	2.37					Ballestracci <i>et al.</i> (21)
	4.232	9.911	177.5	2.34					Rossi <i>et al.</i> (22)
	4.24	9.88	177.6	2.33				293 K, XRD	Grier <i>et al.</i> (2)
	4.2235(5)	9.9871(12)	176.54	2.343				15 K, ND	Grier <i>et al.</i> (2)
	4.2231(3)	9.8962(10)	176.49	2.343	10			5 K, ND	Grier <i>et al.</i> (2)
$\text{CePd}_{2-y}\text{Si}_{2+y}$	4.230	9.873	176.66	2.334	10	-75			Murgai <i>et al.</i> (1)
	4.236	9.874	177.18	2.331	10.5	-57	2.55		Palstra <i>et al.</i> (23)
									Palenzona <i>et al.</i> (24)
$\text{CePd}_{2-x}\text{Mn}_x\text{Si}_2$, $x = 0.25$	4.2033(3)	10.0570(30)	177.69	2.393	18	-24		2 phase, nom. $\text{CePd}_{2.1}\text{Si}_{1.9}$	*
$x = 0.50$	4.1672(2)	10.2099(19)	177.30	2.450	31	-29		2 phase, nom. $\text{CePd}_{1.9}\text{Si}_{2.1}$	*
$x = 0.75$	4.1409(6)	10.3193(27)	176.94	2.492	38	-8		spin flip at 9 kG, 4.2 K	*
$x = 1.00$	4.1202(6)	10.3808(25)	176.23	2.519	87	-5		spin flip at 9 kG, 4.2 K	*
$x = 1.25$	4.0906(8)	10.4423(45)	174.73	2.553	65	43			*
$x = 1.50$	4.0677(11)	10.4826(53)	173.45	2.577	200	132			*
$x = 1.75$	4.0374(7)	10.5045(43)	171.23	2.602	310	269			*
CeMn_2Si_2	4.0098(4)	10.5242(49)	169.22	2.625	385	341	4.12		*
	4.054(5)	10.611(5)	174.4	2.617				373 K, ND	Siek <i>et al.</i> (8)
	4.026(5)	10.568(5)	171.3	2.625	379	330		293 K, ND	Siek <i>et al.</i> (8)
	3.986(5)	10.491(5)	166.7	2.632				78 K, ND, $\mu_{(\text{Mn})} = 2.3\mu_B$	Siek <i>et al.</i> (8)
	4.017	10.508	169.56	2.616					Liang <i>et al.</i> (16)

to the high vapor pressures of manganese during arc melting were controlled by repeated weighing and were compensated by extra amounts of manganese (until losses were below 2%). A part of each alloy button was wrapped in molybdenum foil, sealed in evacuated quartz ampoules, annealed at 800°C for 120 h, and finally quenched in water.

X-ray and (in some cases) metallographic analyses of the $\text{CePd}_{2-x}\text{Mn}_x\text{Si}_2$ alloys proved both the as-cast and the annealed specimens in a practically single-phase condition suggesting a congruent melting behavior throughout the complete pseudobinary alloy system CeMn_2Si_2 - CePd_2Si_2 ; no indications for the existence of a miscibility gap were observed after long-time (700 h) heat treatment of the specimens at 500°C.

Lattice parameters and standard deviations were refined by a least-squares method from room-temperature Guinier-Huber powder photographs ($\text{Cu } K\alpha_1$ radiation, internal standard of 99.9999% pure germanium $a_0 = 5.657906 \text{ \AA}$). X-ray powder intensities were calculated employing the LAZY-PULVERIX program.¹⁷

Magnetic data were recorded in the range $1.5 < T < 300 \text{ K}$ with a Princeton Applied Research vibrating sample magnetometer and in an ac susceptometer. For measurements from 77 to 1000 K a compensating high-precision Faraday pendulum magnetometer (SUS 10, A. Paar KG., Graz, Austria) was used.

The specific-heat measurements were performed in an automated adiabatic calorimeter in the temperature range from 1.5 to 60 K.¹⁸ The calorimeter was calibrated and tested using high-purity (99.999%) copper; the absolute accuracy is estimated to be better than 1% in the low-temperature region and $\pm 3\%$ for $T > 30 \text{ K}$. For electrical resistivity measurements in the temperature range from 4.2 to 300 K a standard four-point technique was employed.

III. RESULTS AND DISCUSSION

A. Structural chemistry

X-ray analysis and metallography of arc-melted samples over the range $\text{CeMn}_x\text{Pd}_{2-x}\text{Si}_2$ proved in all cases ($0 \leq x \leq 2$) congruent melting behavior as well as complete solid solubility, which was also found from lower-temperature heat treatments (800°C and 500°C). Guinier powder patterns for CePd_2Si_2 as well as for Pd-rich alloys with $x < 1$ were completely indexed on the basis of a body-centered tetragonal cell (see Table I) and revealed structural identity with the crystal structure of ThCr_2Si_2 (crystal symmetry $I4/mmm$). Using the atom parameters derived for CeOs_2Si_2 (Ref. 19) and assuming statistical distribution of manganese and palladium atoms on their lattice sites $4d$, we find excellent agreement between the observed and calculated powder intensities. Powder photographs of the alloys with $x = 1.25, 1.5$, and 1.75 reveal a rather small but significant broadening or splitting of some x-ray reflections just discernible by the Guinier technique indicating a lattice distortion towards lower symmetry. This distortion, however, is too small to be successfully refined. Figure 1 represents the variation of the unit-cell volume V and the lattice parameters a and c

for the system CeMn_2Si_2 - CePd_2Si_2 as a function of the Mn-Pd exchange. In the dotted region a distortion of the ThCr_2Si_2 type is observed. The significant positive deviation from Vegard's rule of the c lattice constant may be a hint to a tendency of the solid solution towards a non-linear valence change on the Ce atoms or to an eventual superstructure formation at low temperatures.

B. Magnetic properties, electrical resistivity, and specific heat

Reciprocal gram susceptibilities versus temperature plots for the paramagnetic region up to 1100 K are presented in Fig. 2. The numerical results of the Curie-Weiss extrapolation, the type of ordering, and the corresponding transition temperatures are listed in Table I. Figure 3 represents the susceptibility as a function of

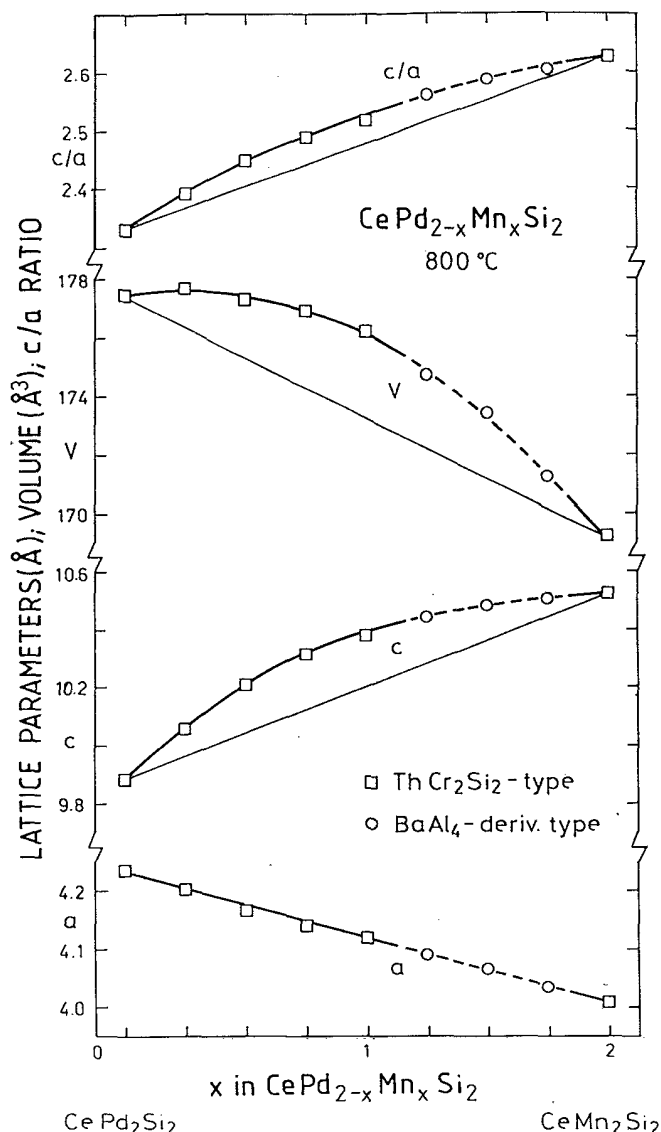


FIG. 1. Lattice parameters a and c , volume V , and c/a ratio vs Mn concentration for $\text{CePd}_{2-x}\text{Mn}_x\text{Si}_2$ ($0 \leq x \leq 2$).

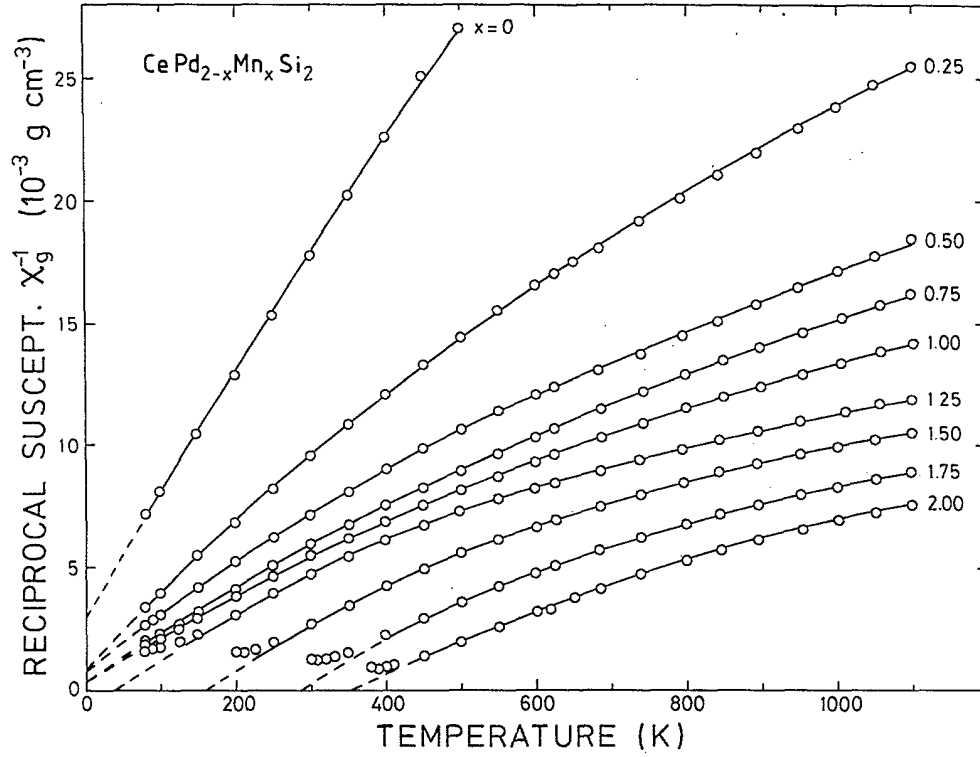


FIG. 2. Reciprocal susceptibility χ^{-1} vs temperature T for $\text{CePd}_{2-x}\text{Mn}_x\text{Si}_2$ ($0 \leq x \leq 2$). Solid lines: calculated values.

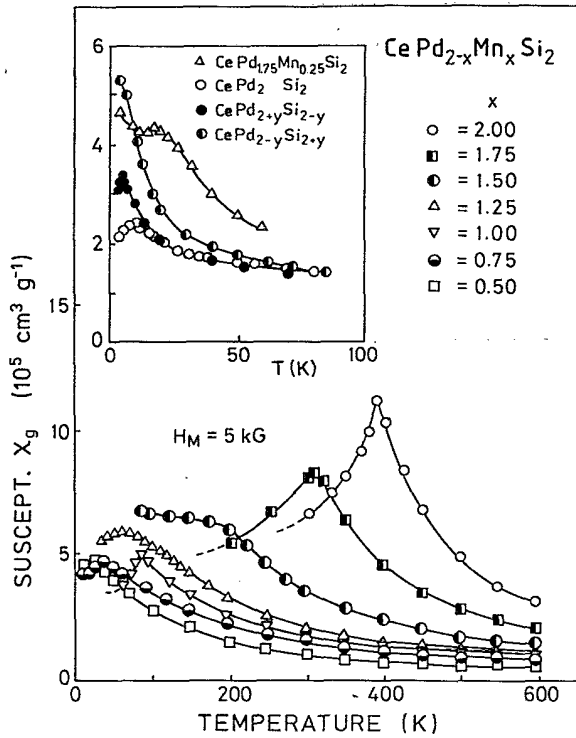


FIG. 3. Susceptibility χ vs temperature T for $\text{CePd}_{2-x}\text{Mn}_x\text{Si}_2$ ($0.5 \leq x \leq 2$). The inset shows the susceptibility vs temperature T for $\text{CePd}_{2-x}\text{Mn}_x\text{Si}_2$ ($x = 0.25$ and 0) and $\text{CePd}_{2\pm y}\text{Si}_{2\mp y}$ ($y = 0.1$).

temperature for $0.5 \leq x \leq 2$. The inset of Fig. 3 shows the low-temperature behavior of the susceptibility of CePd_2Si_2 , some slightly off-stoichiometric samples of $\text{CePd}_{2+y}\text{Si}_{2-y}$ ($y = \pm 0.1$) and of $\text{CePd}_{1.75}\text{Mn}_{0.25}\text{Si}_2$. The magnetic phase diagram of $\text{CePd}_{2-x}\text{Mn}_x\text{Si}_2$ with the paramagnetic Curie temperatures Θ_p , the antiferromagnetic ordering temperatures T_N , and the total magnetic moments μ_{tot} is presented in Fig. 4. The solid symbols

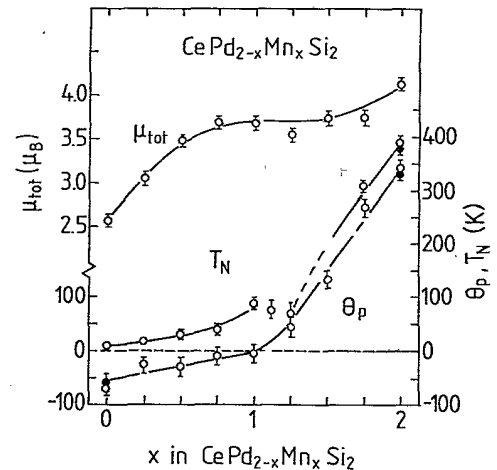


FIG. 4. Magnetic phase diagram of $\text{CePd}_{2-x}\text{Mn}_x\text{Si}_2$ with Θ_p the paramagnetic Curie-Weiss temperatures, T_N the ordering temperatures, and μ_{tot} the total observed paramagnetic moments.

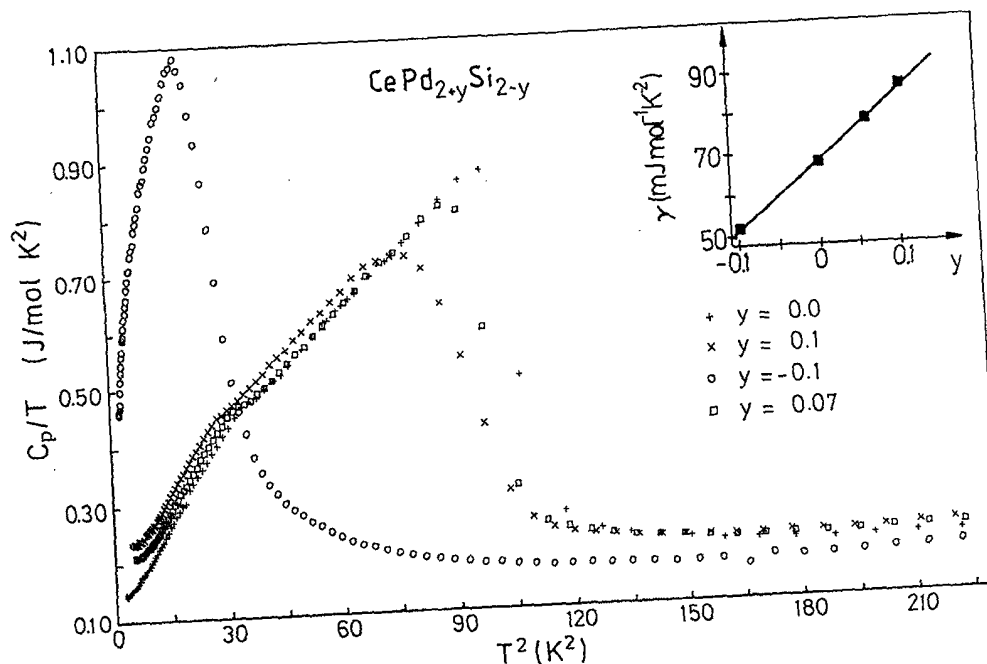


FIG. 5. C_p/T vs T^2 graphs of the specific heat for $\text{CePd}_{2+y}\text{Si}_{2-y}$ ($y = \pm 0.1, 0.07$). The inset shows the Mn concentration dependence of the electronic contribution to the specific heat γ .

represent the values reported by Siek *et al.*⁸ for CeMn_2Si_2 . Paramagnetic moments for the Mn atoms are evaluated assuming a linear decrease of the Ce moment from $2.54\mu_B$ for $x=0$ to $\mu_{\text{Ce}}=0$ for $x=2$. For infinite dilution the Mn moment extrapolates to $5.6\mu_B$, a value close to the free Mn^{2+} moment of $5.9\mu_B$.

1. The boundary phases CePd_2Si_2 and CeMn_2Si_2

$\text{CePd}_2\text{Si}_2\text{W}$ was reported as a Kondo-lattice system exhibiting antiferromagnetic ordering at the Ce sites with an unusually small moment of $0.62\mu_B$ for Ce in the ordered state,² the Néel temperature T_N , and the Kondo temperature T_K exhibiting about the same value of 10 K.³ In fine agreement with the literature we observed the full effective Ce^{3+} moment and a large negative Curie-Weiss temperature of -64 K. The absolute value of the susceptibility at T_N is somewhat lower than reported by Murgai *et al.*¹ Practically no temperature-independent contributions to the paramagnetic susceptibility were observed.

In a previous paper, however, Hiebl *et al.*⁵ did not find magnetic ordering in this compound. Stimulated by this observation in opposition to our results, we investigated the magnetic properties of slightly off-stoichiometric $\text{CePd}_{2+y}\text{Si}_{2-y}$ alloys ($y = \pm 0.1$). The data obtained are presented in the inset of Fig. 3. Together with the results from the low-temperature specific-heat measurements (Fig. 5), it is documented, that any deviation from the exact stoichiometry shifts the Néel temperature T_N to lower temperatures, whether the Pd content increases or decreases. Figure 5 displays specific-heat measurements on $\text{CePd}_{2+y}\text{Si}_{2-y}$ with $y=0.0$ and ± 0.1 in a (C_p/T) -

versus- T^2 representation. Additionally we investigated another remelted sample with a nominal composition $y=0.1$ but with Pd loss during remelting—so the stoichiometry of this off-stoichiometric sample results in $\text{CePd}_{2.07}\text{Si}_{1.93}$. As a rather significant indication for stoichiometry the deviation of the electronic specific-heat coefficient γ from the value for the stoichiometric sample ($67 \text{ mJ mol}^{-1} \text{K}^{-2}$) can be used. The inset in Fig. 5 displays the rather strong and sensitive relation of γ vs y : Starting from $\text{CePd}_{2.1}\text{Si}_{1.9}$ the γ value falls rapidly within $20 \text{ mJ mol}^{-1} \text{K}^{-2}$ with decreasing Pd content. In this context it should be mentioned that the Néel temperature of CePd_2Si_2 was reported to decrease rapidly with applied pressure²⁰ indicating a strong sensitivity to the dominance of the two competing mechanisms in this Kondo-lattice system CePd_2Si_2 , i.e., Kondo and Ruderman-Kittel-Kasuya-Yosida (RKKY) interaction.

For antiferromagnetically ordered CeMn_2Si_2 we observe excellent agreement with the data reported by Siek *et al.*⁸ they did not find hints for a magnetic moment on the cerium sites in the ordered state by means of neutron diffraction. Therefore, the total paramagnetic moment was attributed to the Mn atoms yielding a value of $3.0\mu_B/\text{Mn}$. The large positive Curie-Weiss temperature indicates strong ferromagnetic intraplanar coupling. The temperature-independent contributions to the magnetic susceptibility are rather high ($4 \cdot 10^{-6} \text{ emu/g}$) supporting the suggestion of an antiferromagnetic interplanar coupling mechanism involving conduction electrons. However, the strong deviation from linearity in Fig. 5 may be partly a consequence of magnetic correlation effects.

In this context it is straightforward to mention the employment of Ce L_3 x-ray absorption spectroscopy

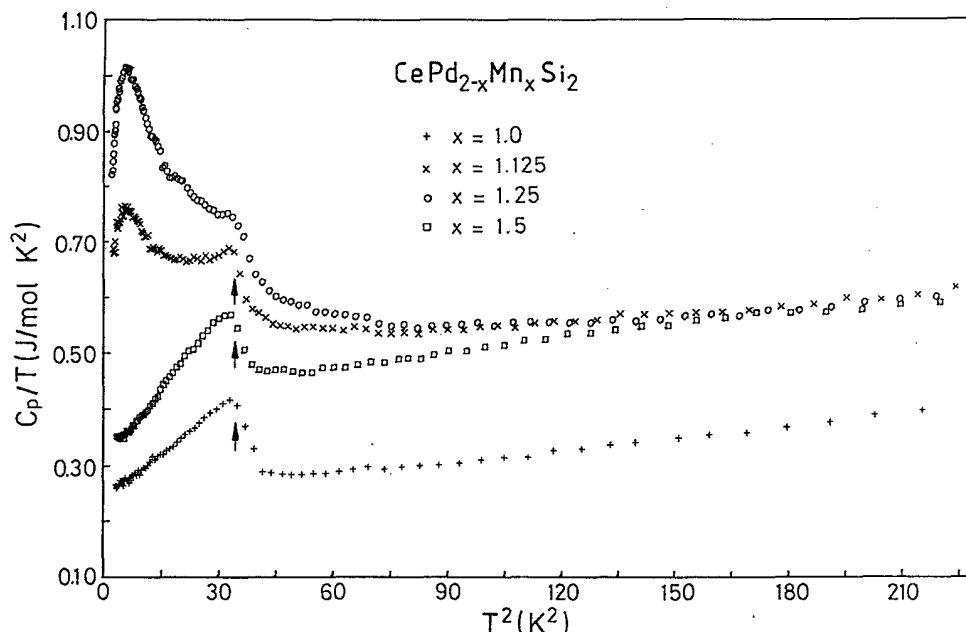


FIG. 6. C_p/T vs T^2 graphs of the specific heat for $\text{CePd}_{2-x}\text{Mn}_x\text{Si}_2$ ($x = 1, 1.125, 1.25, 1.5$). The arrows indicate the magnetic ordering of cerium-oxide impurities.

combination with electrical resistivity, specific-heat, and susceptibility data, Liang *et al.*^{15,16} proved a slightly temperature-dependent mixed-valent Ce state for CeMn_2Si_2 in the presence of a strong 3d magnetic order of the Mn sublattice, which, in turn, is responsible for the effective 4f moment quenching of the weak mixed-valent magnetic contribution. The enhanced Pauli susceptibility (Fig. 2) corresponds to the weak Ce mixed-valent behavior which, similar to the low-temperature Fermi-liquid ground-state system CePd_3 , was also earlier deduced from resistivity and specific-heat measurements.^{15,16}

2. The palladium-manganese substitution

The concentration dependences of the paramagnetic Curie temperatures Θ_p and, to some extent, the ordering temperatures show two approximately linear regions with different slopes for Pd-rich and Mn-rich alloys, respectively (see Fig. 4). With increasing Pd content the magnetic behavior of the $\text{CePd}_{2-x}\text{Mn}_x\text{Si}_2$ compounds, as already shown in Fig. 3, is characterized by a rapid decrease of the magnetization values at T_N with weak indications for antiferromagnetic ordering in the dc susceptibility but with distinct cusps in the ac susceptibility for the alloys with $x = 1.5, 1.25$, and 1.125 . The peaks in the heat capacity for $\text{CePd}_{0.75}\text{Mn}_{1.25}\text{Si}_2$ and $\text{CePd}_{0.875}\text{Mn}_{1.125}\text{Si}_2$ in the intermediate range are due to unresolved magnetic order below 3 K (Fig. 6); this fact is also supported by low-temperature susceptibility measurements revealing an additional magnetic ordering at about 2.5 K. Spin-glass freezing is excluded by the appearance of distinct peaks in both experiments, specific heat and susceptibility. Additionally, at about 6 K, distinct kinks resulting from a foreign Ce-oxide phase ap-

pear. The magnetic order in this intermediate concentration range is not of a conventional type: the strong enhancement of the electronic coefficient γ in the specific heat strongly points to an occurrence of spin fluctuations with growing Mn concentration. Figure 7 presents this strong enhancement of the γ values as well as the magnetic ordering temperatures T_N for $\text{CePd}_{2-x}\text{Mn}_x\text{Si}_2$. The maximum value of about $220 \text{ mJ mol}^{-1} \text{ K}^{-2}$ for the γ enhancement is reached in the intermediate concentration range mentioned above. It is noteworthy that the

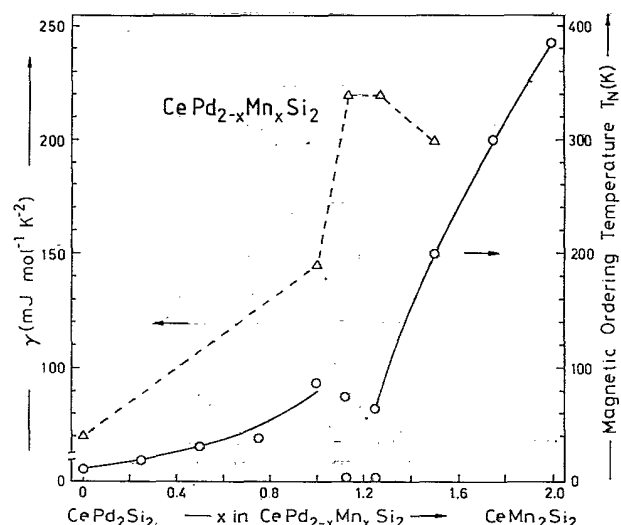


FIG. 7. Magnetic ordering temperatures T_N and γ values for $\text{CePd}_{2-x}\text{Mn}_x\text{Si}_2$.

anomalies in the magnetic behavior occur in samples within the region of lattice distortions of the ThCr_2Si_2 -type structure.

Figure 8 displays the temperature dependence of the resistivity of the alloy $\text{CeMn}_{1.125}\text{Pd}_{0.875}\text{Si}_2$. The correlation of the Kondo minimum in CeMn_2Si_2 to the $3d$ antiferromagnetic ordering has been widely discussed for the $\text{Ce}(\text{Mn}_{1-x}\text{Cr}_x)_2\text{Si}_2$ and the $\text{CeMn}_2(\text{Si}_x\text{Ge}_{1-x})_2$ solid solutions.^{15,16} Similar to $\text{Ce}(\text{Mn}_{1-x}\text{Cr}_x)_2\text{Si}_2$, the anomalous increase of the resistivity with decreasing temperature in $\text{CeMn}_{1.125}\text{Pd}_{0.875}\text{Si}_2$ is attributed to Ce Kondo spin-flip scattering. Furthermore, we observe a still negative temperature coefficient in the resistivity of $\text{CeMn}_{1.125}\text{Pd}_{0.875}\text{Si}_2$ passing through a maximum towards lower temperatures due to coherent Ce scattering such as that typically observed for CePd_3 whereas increasing disorder brought about by the Mn-Pd substitution effectively reduces this coherency effect in $\text{CePd}_{0.875}\text{Mn}_{1.125}\text{Si}_2$ to almost a tenth of that in CeMn_2Si_2 (see Fig. 3).

The anomalous magnetic behavior, the strong γ enhancement, and the predicted appearance of spin fluctuations open a catalogue of questions in which way (i) the magnetic ordering changes from the [001] Mn to the [110] Ce antiferromagnetic ordering and (ii) the individual paramagnetic moments can be reasonably arranged to yield the observed total susceptibility values. As shown in Fig. 4, the total paramagnetic moment μ_{tot} remains more or less constant as soon as 25% of the Pd is substituted by Mn.

While the Ce moments gradually decrease on successive Pd by Mn substitution, the coupling of the Ce moments via $4f$ electron interactions is strongly influenced by the substitution of the $3d$ by the $4d$ metal. In the transition region ($1.0 < x < 1.5$) in correspondence with the orthorhombic lattice distortion the magnetic behavior (as seen from Fig. 7) is characterized by Ce valence instabilities in combination with the gradual development of antiferromagnetic [001] order on the Mn sublattice, thus the unresolved order at low temperatures may be reluctantly

attributed to the magnetic order of the reduced Ce moments.

From the qualitative behavior of the magnetization curves, one may infer that the Mn [001] ordering degenerates rapidly with antiferromagnetic ordering around 60–70 K and unresolved magnetic order occurs below 3 K for concentrations $1.25 \leq x \leq 1.5$. This is probably the region where the orientation of the magnetic moments switches from the [001] to the [110] orientation observed for the CePd_2Si_2 compound. Magnetization measurements up to 18 kG at 4.2 K revealed a spin-flip (9 kG) behavior for $x = 0.5$ and 0.75 only, i.e., already in the Pd-rich region, where the smooth increase of the ordering temperatures T_N with decreasing Pd concentration indicates a more or less continuous change of the magnetic behavior. Therefore, we cannot conclusively suggest a particular mechanism for the possible reorientation of the spin axis in the transition region $1.0 < x < 1.5$. For both compositions $x = 1.0$ and 1.5 , no additional unresolved magnetic order could be detected in the low-temperature regime ($1.5 < T < 10$ K). It seems that the ordering in the Pd-rich region is dominated by the [110] spin direction as observed in the CePd_2Si_2 samples. Obviously, the magnetic ordering is enhanced in this region by the Mn substitution, eventually precluding any different orientation for the Mn and Ce spins, respectively.

Together with the observed enhancement of the γ value in the intermediate concentration range, the reduction of the entropy at the transition temperature, which attains about $4 \text{ J mol}^{-1} \text{ K}^{-1}$ for CePd_2Si_2 and does not reach the theoretical value for a spin- $\frac{1}{2}$ system [$S = R \ln(2J + 1) = 5.76 \text{ J mol}^{-1} \text{ K}^{-1}$], is a strong indication for a Kondo-like screening of the magnetic moments. Grier *et al.*³ claimed a strong spin-fluctuation system for CePd_2Si_2 with a temperature dependence of the electrical resistivity pointing to a Kondo scattering mechanism. This indication is directly supported by the electrical resistivity and specific-heat measurements presented in this work, especially in the concentration range where the γ value is strongly enhanced.

IV. CONCLUSION

Magnetic properties of the $\text{CePd}_{2+y}\text{Si}_{2-y}$ ($y = \pm 0.1$) were observed to be rather sensitive to minor deviations from the stoichiometry, which was also documented by specific-heat measurements: The Néel temperature is shifted to lower temperatures as the Pd content deviates from the stoichiometry.

The magnetic phase diagram of $\text{CePd}_{2-x}\text{Mn}_x\text{Si}_2$ reveals two regions of different magnetic interactions; $4f$ magnetism dominates in the Pd-rich alloys, where Mn substitution enhances $4f$ antiferromagnetism, while $3d$ magnetism is rapidly suppressed on Mn-Pd substitution. In the intermediate range unresolved magnetic order occurs additionally below 3 K for $\text{CePd}_{0.75}\text{Mn}_{1.25}\text{Si}_2$ and $\text{CePd}_{0.875}\text{Mn}_{1.125}\text{Si}_2$. The valence of Ce in CePd_2Si_2 is close to 3. The magnetic order is not of a conventional type since spin fluctuations appear to be strong; the high electronic specific-heat coefficient γ ($\sim 220 \text{ mJ mol}^{-1} \text{ K}^{-2}$) and the reduced entropy of the antiferro-

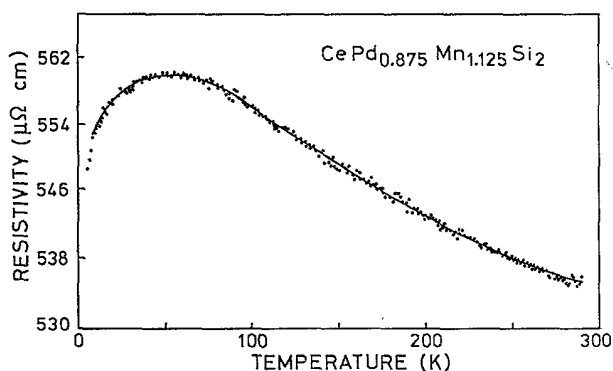


FIG. 8. Electrical resistivity of $\text{CeMn}_{1.125}\text{Pd}_{0.875}\text{Si}_2$ from 4.2 to 300 K. The solid line serves as a guide to the eye.

magnetic transition ($4 \text{ J mol}^{-1} \text{ K}^{-1}$) for CePd_2Si_2 is a consequence of the Kondo scattering mechanism in this alloy regime. The γ values in the pseudobinary system remain high due to the intermediate valence as a consequence of the transition from nearly Ce^{3+} in CePd_2Si_2 to almost Ce^{4+} in CeMn_2Si_2 , going hand in hand with a change from $4f$ to $3d$ magnetism.

ACKNOWLEDGMENTS

P.R. expresses his gratitude to the Hochschuljubiläumsstiftung der Stadt Wien for the KD-530-type microdensitometer and the MTN-50 balance and to the Austrian Science Foundation (FWF Project No. P5279). Three of us (G.H., N.P. and G.S.) wish to acknowledge a grant from the Austrian National Bank (Project No. 3492).

- ¹V. Murgai, S. Raaen, L. C. Gupta, and R. D. Parks, in *Valence Instabilities*, edited by P. Wachter and H. Boppart (North-Holland, Amsterdam, 1982), p. 537.
- ²B. H. Grier, J. M. Lawrence, V. Murgai, and R. D. Parks, *Phys. Rev. B* **29**, 2664 (1984).
- ³B. H. Grier, J. M. Lawrence, S. Horn, and J. D. Thompson, *J. Phys. C* **21**, 1099 (1988).
- ⁴S. Quezel, J. Rossat-Mignod, B. Chevalier, P. Lejay, and J. Etourneau, *Solid State Commun.* **49**, 685 (1984).
- ⁵K. Hiebl, C. Horvath, and P. Rogl, *J. Less Common Met.* **117**, 375 (1986).
- ⁶J. Leciejewicz and A. Szytula, in *Universitas Iagellonica Acta Scientiarum Literarumque DCCCXXXI*, edited by B. Sredniawa (Panstwowe Wydawnictwo Naukowe, Warszawa, 1987), pp. 1–99.
- ⁷P. Rogl, *Phase Equilibria in Ternary and Higher Order Systems Containing Rare Earth Elements and Silicon*, in Vol. 7 of the *Handbook on the Physics and Chemistry of Rare Earths*, edited by K. A. Gschneidner, Jr. and L. Eyring (North-Holland, Amsterdam, 1984), pp. 1–264.
- ⁸S. Siek, A. Szytula, and J. Leciejewicz, *Phys. Status Solidi A* **46**, K101 (1978).
- ⁹Z. Ban, L. Omejec, A. Szytula, and Z. Tomkowicz, *Phys. Status Solidi A* **27**, 333 (1975).
- ¹⁰J. Leciejewicz, S. Siek, and A. Szytula, *J. Magn. Magn. Mater.* **40**, 265 (1984).
- ¹¹B. Rupp, P. Rogl, and F. Hulliger, *J. Less Common Met.* **135**, 113 (1987).
- ¹²K. Hiebl, C. Horvath, P. Rogl, and M. J. Sienko, *Z. Phys. B* **56**, 201 (1984).
- ¹³P. Rogl, K. Hiebl, and G. Wiesinger, *J. Mater. Sci.* **24**, 2250 (1989).
- ¹⁴R. A. Neifeld, M. Croft, T. Mihalisin, C. U. Segre, M. Madigan, M. S. Torikachvili, M. B. Maple, and L. E. DeLong, *Phys. Rev. B* **32**, 6928 (1985).
- ¹⁵G. Liang, I. Perez, D. DiMarzio, M. Croft, D. C. Johnston, N. Anbalagan, and T. Mihalisin, *Phys. Rev. B* **37**, 5970 (1988).
- ¹⁶G. Liang, M. Croft, D. C. Johnston, N. Anbalagan, and T. Mihalisin, *Phys. Rev. B* **38**, 5302 (1988).
- ¹⁷K. Yvon, W. Jeitschko, and E. Parthé, LAZY-PULVERIX program, *J. Appl. Crystallogr.* **10**, 7 (1977); updated interactive VAX-VMS version, B. Rupp, University of Vienna, 1985.
- ¹⁸C. Schmitzer, Ph.D. thesis, Technical University of Vienna, 1985.
- ¹⁹C. Horvath and P. Rogl, *Mater. Res. Bull.* **18**, 443 (1983).
- ²⁰J. D. Thompson, R. D. Parks, and H. Borges, *J. Magn. Magn. Mater.* **54-57**, 377 (1986).
- ²¹R. Ballestracci, *C. R. Acad. Sci. Paris, Ser. B* **282**, 291 (1976).
- ²²D. Rossi, R. Marazza, and R. Ferro, *J. Less. Common. Met.* **66**, P17 (1979).
- ²³T. T. M. Palstra, Ph.D. thesis, Rijksuniversiteit Leiden, Netherlands, 1986.
- ²⁴A. Palenzona, S. Cirafici, and F. Canepa, *J. Less Common. Met.* **135**, 185 (1987).